PROCEEDINGS OF SCIENCE

Boron flux in cosmic rays and its flux ratio to primary species measured with CALET on the International Space Station

P. Maestro[a,b,*] **and Y. Akaike**[c,d] **for the CALET collaboration**

[a] *Department of Physical Sciences, Earth and Environment, University of Siena, via Roma 56, 53100 Siena, Italy,*

[b] *INFN Sezione di Pisa, Polo Fibonacci, Largo B. Pontecorvo, 3 - 56127 Pisa, Italy*

[c] *Waseda Research Institute for Science and Engineering, Waseda University, 17 Kikuicho, Shinjuku, Tokyo 162-0044, Japan*

[d] *JEM Utilization Center, Human Spaceflight Technology Directorate, Japan Aerospace Exploration Agency, 2-1-1 Sengen, Tsukuba, Ibaraki 305-8505, Japan*

E-mail: maestro@unisi.it

We present the measurement of the energy spectrum of the boron flux in cosmic rays based on the data collected by the CALorimetric Electron Telescope (CALET) during 7.25 years of operation on the International Space Station. The energy spectrum is measured from 8.4 GeV/n to 3.8 TeV/n with an all calorimetric instrument with a total thickness corresponding to 1.3 nuclear interaction length and equipped with charge detectors capable of single element resolution. The observed boron flux shows a spectral hardening at the same transition energy $E_0 \sim 200$ GeV/n of the carbon and oxygen spectra, though B flux has a different energy dependence with respect to C and O. Within the limitations of our data's present statistical significance, the boron spectral index change is found to be slightly larger than that of carbon and oxygen, which are similar. A corresponding break in the energy dependence of the B/C and B/O flux ratios also supports the idea that the secondary cosmic rays exhibit a stronger hardening than primary ones. Moreover, interpreting our data with a Leaky Box model, we argue that the trend of the energy dependence of the B/C and B/O ratios in the TeV/n region could suggest a possible presence of a residual propagation path length, compatible with the hypothesis that a fraction of secondary B nuclei can be produced near the cosmic-ray source.

38th International Cosmic Ray Conference (ICRC2023)
26 July - 3 August, 2023
Nagoya, Japan

ICRC2023
38th International Cosmic Ray Conference
The Astroparticle Physics Conference

*Speaker

PoS(ICRC2023)058

1. Introduction

Secondary cosmic-ray (CR) nuclei, such as Li, Be, B, are produced by the spallation reactions of primary CR, injected and accelerated in astrophysical sources, with nuclei of the interstellar medium (ISM). Measurements of the secondary-to-primary abundance ratios (as B/C or B/O) make it possible to probe galactic propagation models and constrain their parameters, since they are expected to be proportional at high energy to the average amount of material λ traversed by CR in the Galaxy, which in turn is inversely proportional to the CR diffusion coefficient D. Earlier measurements [1–5] indicate that λ decreases as a power-law of the energy per nucleon $\lambda \propto E^{-\delta}$, where δ is the diffusion spectral index. The recently observed hardening in the spectrum of CR of different nuclear species [6–11] can be explained as due to subtle effects of CR transport including: an energy-dependent diffusion coefficient [12–14]; the possible re-acceleration of secondary particles crossing a supernova shock during propagation [15]; and/or the production of a small fraction of secondaries by interactions of primary nuclei with matter (source grammage) inside the acceleration region [16–18]. To study these phenomena, a precise determination of the energy dependence of λ is necessary, which can be obtained by extending the measurements of secondary CR in the TeV/n region with high statistics and low systematic uncertainties.
New direct measurements of the energy spectrum of boron and its flux ratio to carbon and oxygen in the energy range from 8.4 GeV/n to 3.8 TeV/n are presented here, based on the data collected by CALET [19, 20] from Oct. 13, 2015 to Dec. 31, 2022 aboard the International Space Station (ISS).

2. Detector

The CALET instrument comprises a CHarge Detector (CHD), a finely segmented pre-shower IMaging Calorimeter (IMC), and a Total AbSorption Calorimeter (TASC).
The IMC consists of 7 tungsten plates interspaced with eight double layers of scintillating fibers, arranged along orthogonal directions. Fiber signals are used to reconstruct the CR arrival direction by applying a combinatorial Kalman filter [21]. The estimated error for light nuclei is $\sim 0.1^{\circ}$, while the spatial resolution of the impact point on the CHD is $\sim$220 μm.
The CHD, located above the IMC, is comprised of two hodoscopes (CHDX, CHDY) made of 14 plastic scintillator paddles each, arranged perpendicularly to each other. The particle identification is based on the charge values reconstructed, on an event-by-event basis, from the measured energy deposit in each CHD layer (Z_{CHDX}, Z_{CHDY}) and the average of the dE/dx samples along the track in the top half of IMC layers (Z_{IMC}) [7]. The CHD can resolve individual chemical elements from $Z = 1$ to 40, while the saturation of the fiber signals limits the IMC charge measurement to $Z \lesssim 14$. The charge resolution is $\sim 0.15\,e$ for CHD ($0.24\,e$ for IMC) in the elemental range from B to O.
The TASC is made of 12 layers of lead-tungstate bars, each read out by photosensors and a front-end electronics spanning a dynamic range $> 10^6$. The total thickness of the instrument is equivalent to 30 radiation lengths and 1.3 proton nuclear interaction lengths.
A long campaign of beam tests were carried out at the CERN-SPS to calibrate the detector with protons, electrons and ion fragments [7, 22]. Detailed Monte Carlo (MC) simulations of the instrument have been performed, based on the EPICS package [23]. Independent simulations based on Geant4 10.5 [24] are used to assess the systematic uncertainties.

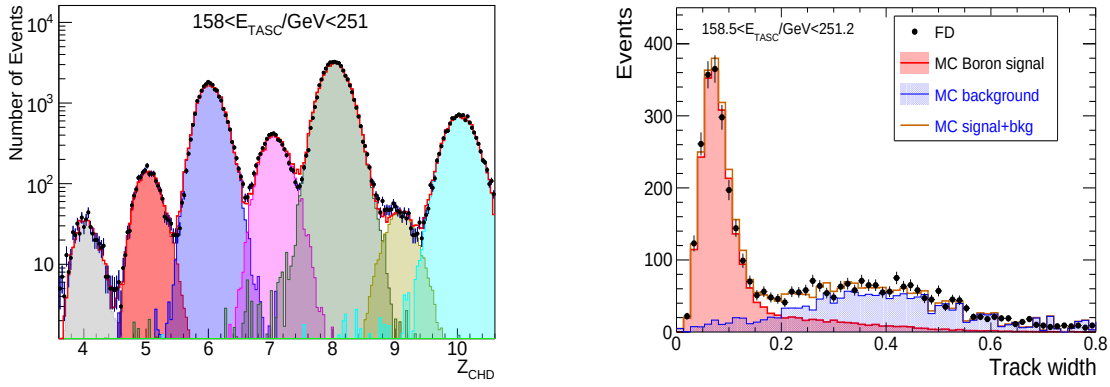

(a) (b)

Figure 1: (*a*) Z_{CHD} (mean value of Z_{CHDX} and Z_{CHDY}) distribution measured in FD in the energy interval $158 < E_{\mathrm{TASC}}/\mathrm{GeV} < 251$, compared with MC simulations. (*b*) Track width (TW) of B events selected in the same energy bin by means of CHD only, with superimposed the MC distributions of B and background nuclei (mainly proton, He, C).

3. Data analysis

We have analyzed flight data (FD) collected in 2554 days of CALET operation aboard the ISS. Raw data are corrected for non-uniformity in light output, time and temperature dependence, and gain differences among the channels by using penetrating protons and He particles selected by a dedicated trigger mode [25].

B, C and O candidates are searched for among events selected by the onboard high-energy (HE) shower trigger, which requires the coincidence of the summed signals of the last two IMC double layers and the top TASC layer. The total observation live time for the HE trigger is $T = 5.28 \times 10^4$ hours, corresponding to 86% of the total observation time. The reconstructed events are required to traverse the whole detector (i.e., from CHD top to TASC bottom, with 2 cm clearance from the edges of the TASC top layer) and be contained inside a fiducial region, with a geometric factor $S\Omega$ ~510 cm^{2}sr. Events entering the instrument from lateral sides and erroneously reconstructed inside the fiducial acceptance are rejected, with very high efficiency, by means of topological cuts based on the the shape of the longitudinal and lateral shower profiles.

B, C and O candidates are identified by applying window charge cuts of half-width 0.45 e to the charge peaks in the Z_{CHD} distribution (Fig. 1(a)), obtained after requiring that the three independent charge measurements Z_{CHDX}, Z_{CHDY} and Z_{IMC} are compatible with each other. An additional cut on the track width[1] (TW < 0.2) is applied to reject particles undergoing a charge-changing nuclear interaction in the upper part of the instrument, as shown in Fig. 1(b). A fraction (~ 8%) of events in the final candidate samples are discarded in the analysis, since they have reconstructed trajectories pointing to obstacles (e.g. ISS solar panels, robotic arms) partially shielding the field-of-view of CALET (at angles > 45°).

With this selection procedure about 2.3×10^5 B, 1.1×10^6 C and 2×10^6 O nuclei are identified. The energy spectrum for each species is obtained from the distribution of the TASC energy deposit sum

[1] defined as the difference, normalized to the particle charge, between the total energy deposited in the clusters of nearby fibers crossed by the reconstructed track and the sum of the fiber signals in the cluster cores.

($E_{\rm TASC}$) as follows:

$$\Phi(E) = \frac{N(E)}{\Delta E\ \varepsilon(E)\ S\Omega\ T} \tag{1}$$

$$N(E) = U\left[N_{obs}(E_{\rm TASC}) - N_{bg}(E_{\rm TASC})\right] \tag{2}$$

where: ΔE is the energy bin width; E the kinetic energy per nucleon calculated as the geometric mean of the lower and upper bounds of the bin; $N(E)$ the bin content in the unfolded distribution; $\varepsilon(E)$ the total selection efficiency [7, 26]; $U()$ the iterative unfolding procedure [27] which is applied to correct the $E_{\rm TASC}$ distribution for significant bin-to-bin migration effects (due to the limited TASC energy resolution, $\sim$ 30%) and infer the primary particle energy; $N_{obs}(E_{\rm TASC})$ the bin content of the observed energy distribution (including background); $N_{bg}(E_{\rm TASC})$ the bin content of background events in the observed energy distribution. The total background contamination of B is $\sim$ 1% for $E_{\rm TASC} < 10^2$ GeV and grows logarithmically with $E_{\rm TASC}$ above 10^2 GeV, approaching $\sim$ 7% at 1.5 TeV. The background contamination is < 1% in C and O spectra. The isotopic composition of boron is assumed as $^{11}{\rm B}/(^{10}{\rm B} + ^{11}{\rm B}) = 0.7$ for all energies.

Several sources of systematic uncertainties were investigated, including trigger efficiency, charge identification, energy scale correction, unfolding procedure, MC simulations, B isotopic composition, and background subtraction. The main contribution comes from the different MC simulations (EPICS vs. Geant4) used in the analysis, which produce similar selection efficiencies but energy response matrices that differ significantly in the low- and high-energy regions. The resulting fluxes for B (C, O) show discrepancies not exceeding 6% (10%, 4.5%) below 20 GeV/n and 12% (10%, 12%) above 300 GeV/n, respectively. Breakdown of systematic errors can be found in [26].

4. Results

The energy spectra of B, C and O and their flux ratios measured with CALET are shown in Fig. 2 and compared with earlier results from space-based [1, 2, 5, 6, 11] and balloon-borne [3, 4, 28, 29] experiments. The B spectrum is consistent with that of PAMELA [5] and most of the earlier experiments but the absolute normalization is in tension with that of AMS-02, as already pointed out by our previous measurements of the C, O and Fe fluxes [7, 30]. However we notice that the B/C and B/O ratios are consistent with the ones measured by AMS-02. The C and O spectra shown here are based on a larger dataset but they are consistent with our earlier result [7, 26] and includes an improved assessment of systematic errors.

Figure 3 shows the fits to CALET B and the combined C and O data with a double power-law function (DPL)

$$\Phi(E) = \begin{cases} c\left(\frac{E}{\rm GeV}\right)^{\gamma} & E \le E_0 \\ c\left(\frac{E}{\rm GeV}\right)^{\gamma}\left(\frac{E}{E_0}\right)^{\Delta\gamma} & E > E_0 \end{cases} \tag{3}$$

where c is a normalization factor, γ the spectral index, and $\Delta\gamma$ the spectral index change above the transition energy E_0. A single power-law function (SPL) is also shown for comparison, where $\Delta\gamma = 0$ is fixed in Eq. (3) and the fit is limited to data points with $25 < E < 200$ GeV/n and extrapolated above. The simultaneous DPL fit to the C and O spectra (with common parameters, except normalizazion) in the energy range [25, 3800] GeV/n yields $\gamma_{CO} = -2.66 \pm 0.02$, $\Delta\gamma_{CO} = 0.19 \pm 0.04$, and $\tilde{E}_0 = (260 \pm 50)$ GeV/n confirming our first results reported in Ref. [7]. Fitting

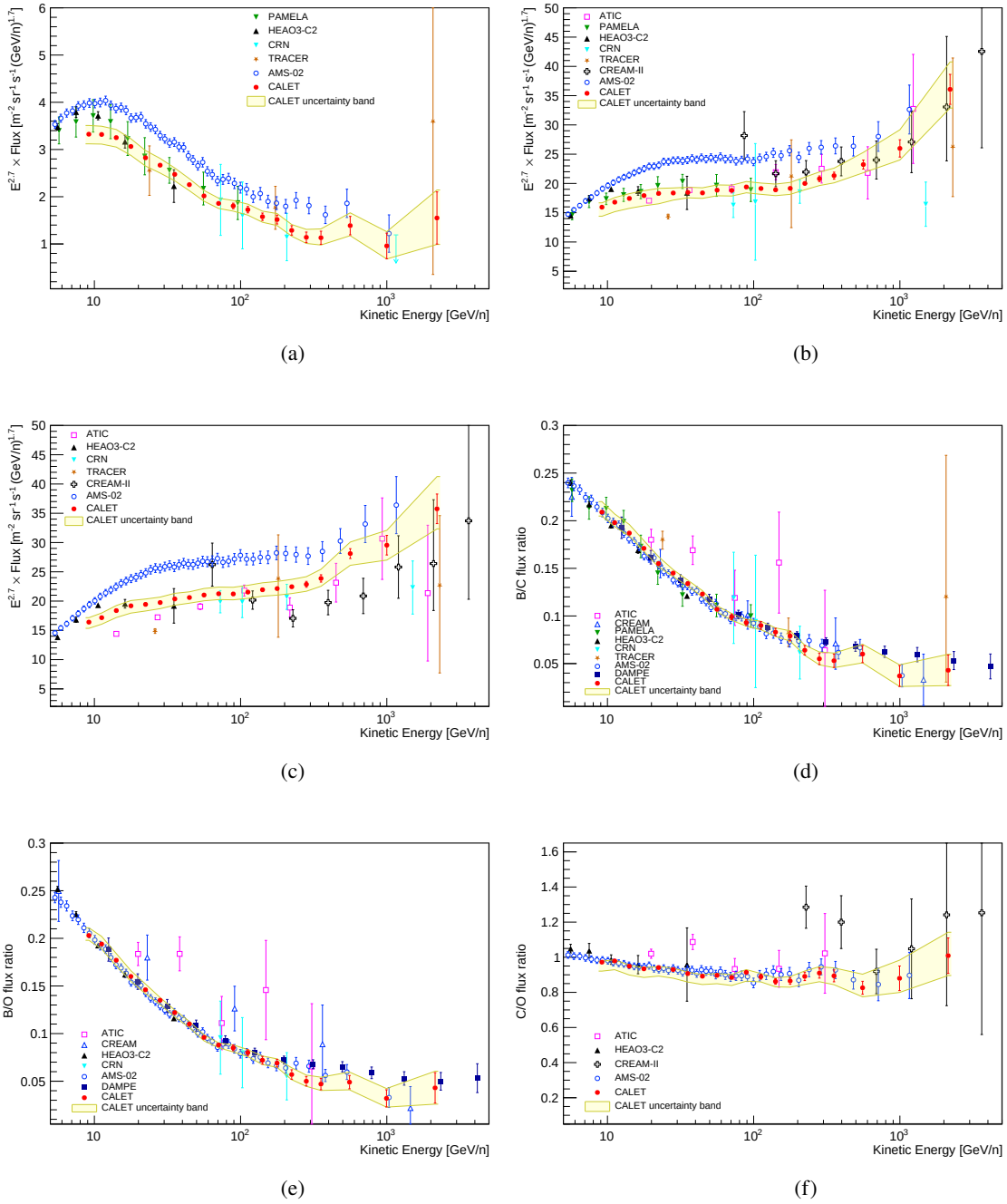

Figure 2: CALET (a) boron, (b) carbon and (c) oxygen flux (multiplied by $E^{2.7}$) and ratio of (d) boron to carbon, (e) boron to oxygen, and (f) carbon to oxygen as a function of kinetic energy per nucleon E. Error bars of CALET data (red) represent the statistical uncertainty only, while the yellow band indicates the quadratic sum of statistical and systematic errors. Also plotted are other direct measurements [1–6, 11, 28, 29].

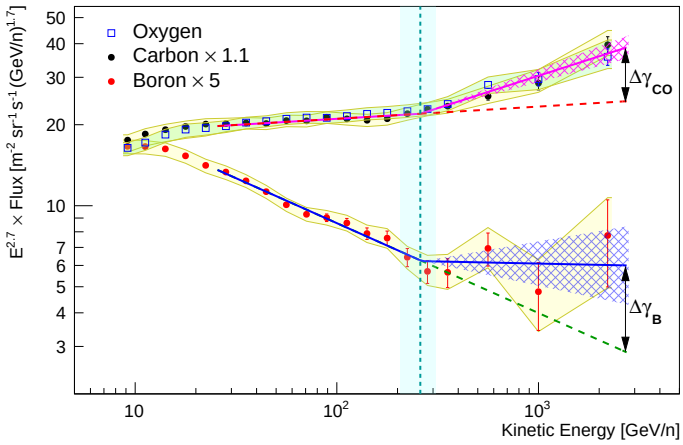

Figure 3: CALET B (red dots), C (black dots) and O (blue open squares) energy spectra are fitted with DPL functions (magenta line for the fit to the combined C and O data, blue line for B). The B spectrum is multiplied by a factor 5 to overlap the low-energy region of the C and O spectra. Error bars represent the statistical uncertainty only, while the yellow (green for O) bands indicate the quadratic sum of statistical and systematic errors. The dashed lines represent the extrapolation of a SPL function fitted to data in the energy range [25, 200] GeV/n. The magenta (blue) cross-shaded area shows the $\pm1\sigma$ error interval of $\Delta\gamma$ from the fit to C and O (B) data. The fitted value of the transition energy $\tilde{E}_0$ is represented by the vertical cyan dashed line, while the the cyan band shows its $\pm1\sigma$ error interval.

the B flux with E_0^B fixed to $\tilde{E}_0$, yields $\gamma_B = -3.03 \pm 0.03$ and $\Delta\gamma_B = 0.32 \pm 0.14$ with χ^2/d.o.f. = 5.2/11. The energy spectra are clearly different as expected for primary and secondary CR, and the fit results seem to indicate, albeit with low statistical significance, that the flux hardens more for B than for C and O above 200 GeV/n. A similar indication also comes from the simultaneous fit to the B/C and B/O flux ratios (Fig. 4(a)). Fitting with SPL functions in the energy range [25, 3800] GeV/n, yields a mean spectral index $\Gamma = -0.376 \pm 0.014$ (χ^2/d.o.f. = 19/27). However a DPL functions provide a better fit suggesting a trend of the data towards a flattening of the B/C and B/O ratios at high energy, with a spectral index change $\Delta\Gamma = 0.22 \pm 0.10$ (χ^2/d.o.f. = 15/26) above $\tilde{E}_0$, which is left as a fixed parameter in the fit. This result is consistent with that of AMS-02 [6], and supports the hypothesis that secondary B exhibits a stronger hardening than primaries C and O, although no definitive conclusion can be drawn due to the large uncertainty in $\Delta\Gamma$ given by our present statistics.

Within the "leaky-box" (LB) approximate modeling of the particle transport in the Galaxy [4], the B/C and B/O flux ratios can be expressed as

$$\frac{\Phi_B(E)}{\Phi_C(E)} = \frac{\lambda(E)\lambda_B}{\lambda(E)+\lambda_B}\left[\frac{1}{\lambda_{C\to B}} + \frac{\Phi_O(E)}{\Phi_C(E)}\frac{1}{\lambda_{O\to B}}\right]$$
$$\frac{\Phi_B(E)}{\Phi_O(E)} = \frac{\lambda(E)\lambda_B}{\lambda(E)+\lambda_B}\left[\frac{1}{\lambda_{O\to B}} + \frac{\Phi_C(E)}{\Phi_O(E)}\frac{1}{\lambda_{C\to B}}\right] \quad (4)$$

where λ_B is the interaction length of B nuclei with matter of the ISM and $\lambda_{C\to B}$ ($\lambda_{O\to B}$) is the average path length for a nucleus C (O) to spall into B. The spallation path lengths are calculated using the parametrization of the total and partial charge changing cross sections provided in Ref. [31], assuming that they are constant above a few GeV/n, and an ISM composition of 90% hydrogen and 10% helium. The small contribution to the B flux due to the spallation of heavier primary nuclei (Ne, Mg, Si, Fe) is neglected. The LB model describes the diffusion of CR in the Galaxy with

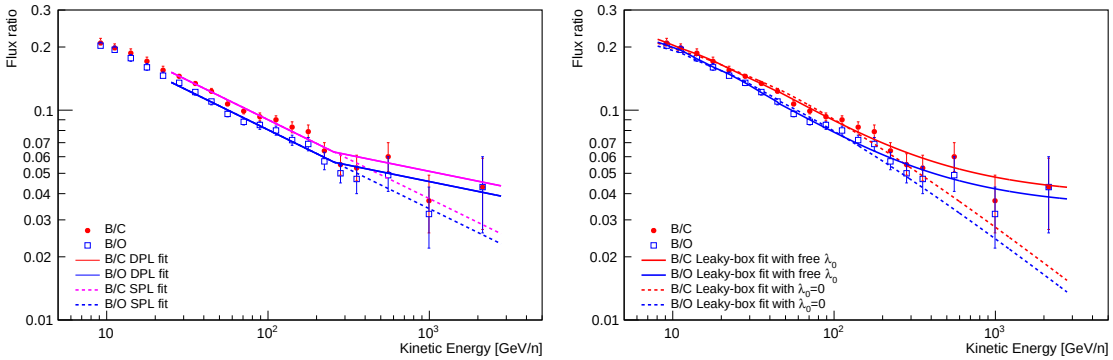

(a) h (b)

Figure 4: Simultaneous fit of the CALET B/C and B/O flux ratios with: (a) SPL (dashed lines) and DPL (solid lines) functions; (b) a leaky-box model (Eq. (4)) leaving the λ_0 parameter free to vary (solid line) or fixing it at zero (dashed line), respectively. The error bars are the quadratic sum of the statistical and systematic uncertainties.

a mean escape path length $\lambda(E)$ which, according to presently available direct measurements, is parametrized as a power-law function of kinetic energy E as follows:

$$\lambda(E) = kE^{-\delta} + \lambda_0 \tag{5}$$

where δ is the diffusion coefficient spectral index. A residual path length λ_0 is included in the asymptotic behavior of λ, which can be interpreted as the amount of matter traversed by CR inside the acceleration region (source grammage). Fitting simultaneously our B/C and B/O data to Eq. (4) (Fig. 4(b)) using our measurement for $\Phi_C(E)/\Phi_O(E)$, the best fit values without the source grammage term ($\lambda_0 = 0$) are: $k = 13.1 \pm 0.2$ g/cm^2, $\delta = 0.61 \pm 0.01$ (χ^2/d.o.f. = 58.3/38). Leaving instead λ_0 free to vary in the LB fit, we obtain: $k = 13.0 \pm 0.3$ g/cm^2, $\delta = 0.81 \pm 0.04$, $\lambda_0 = 1.17 \pm 0.16$ g/cm^2 (χ^2/d.o.f. = 17.9/37). The significance of a non-null value of λ_0 exceeds the 5σ level, suggesting that the residual path length could be the cause of the apparent flattening of the B/C and B/O ratios at high energy. The best fit values of δ and λ_0 are compatible with the ones obtained from a combined analysis of the B/C data from earlier experiments [4], and with the predictions of some recent theoretical works [15, 18].

5. Conclusion

The CR boron spectrum has been measured by CALET up to 3.8 TeV/n using 87 months of data collected aboard the ISS. Our observations show that, despite their different energy dependence, the boron flux exhibits spectral hardening occurring at approximately the same energy as that of carbon and oxygen. Within the limitations of our data's present statistical significance, the boron spectral index change is found to be slightly larger than that of carbon and oxygen. This trend seems to corroborate the hypothesis that secondary CR harden more than the primaries, as recently reported by AMS-02 [6]. Interpreting our data with a LB model, we argue that the trend of the energy dependence of the B/C and B/O ratio in the TeV/n region could suggest a possible presence of a residual propagation path length, compatible with the hypothesis that a fraction of secondary B nuclei can be produced near the CR source.

Acknowledgments

We gratefully acknowledge JAXA's contributions to the development of CALET and to the operations onboard the International Space Station. The CALET effort in Italy is supported by ASI ander Agreement No.2013-018-R.0 and its amendments. The CALET effort in the United States is supported by NASA through Grants No. 80NSSC20K0397, No. 80NSSC20K0399, and NNH18ZDA001N-APRA18-0004.

References

[1] J. J. Engelmann *et al.* (HEAO-3), Astron. Astrophys. **233**, 96 (1990).

[2] S.P. Swordy *et al.*, Astrophys. J. **349**, 625 (1990).

[3] H. S. Ahn *et al.* (CREAM), Astroparticle Phys. **30**, 133 (2008).

[4] A. Obermeier *et al.* (TRACER), Astrophys. J. **752**, 69 (2012).

[5] O. Adriani *et al.* (PAMELA), Astrophys. J. **93**, 791 (2014).

[6] M. Aguilar *et al.* (AMS), Phys. Rev. Lett. **117**, 231102 (2016); Phys. Rev. Lett. **120**, 021101 (2018); Physics Reports **894**, 1 (2021).

[7] O. Adriani *et al.* (CALET), Phys. Rev. Lett. **125**, 251102 (2020).

[8] O. Adriani *et al.* (CALET), Phys. Rev. Lett. **129**, 101102 (2022).

[9] Q. An *et al.* (DAMPE), Sci. Adv. **129**, eaax3793 (2019).

[10] F. Alemanno *et al.* (DAMPE), Phys. Rev. Lett. **126**, 201102 (2021).

[11] F. Alemanno *et al.* (DAMPE), Science Bullettin **67**, 2162 (2022).

[12] G. Jóhannesson *et al.*, Astrophys. J. **824**, 16 (2016).

[13] R. Aloisio, P. Blasi, and P.D. Serpico, A&A **A95**, 583 (2015).

[14] N. Tomassetti, Astrophys. J. Lett. **752**, L13 (2012).

[15] M. Korsmeier, and A. Cuoco, Phys. Rev. D **103**, 103016 (2021).

[16] V. Bresci, E. Amato, P. Blasi, and G. Morlino, Mon. Not. R. Astron. Soc. **488**, 2068 (2019).

[17] R. Cowsik, and B. Burch, Phys. Rev. D **82**, 023009 (2010).

[18] C. Evoli, R. Aloisio, and P. Blasi, Phys. Rev. D **99**, 103023 (2019).

[19] O. Adriani *et al.* (CALET), Phys. Rev. Lett. **120**, 261102 (2018).

[20] O. Adriani *et al.* (CALET), Phys. Rev. Lett. **122**, 181102 (2019).

[21] P. Maestro and N. Mori (CALET), in *Proceedings of Science (ICRC2017) 208* (2017).

[22] Y. Akaike (CALET), in *Proceedings of Science (ICRC2015) 613* (2015).

[23] K. Kasahara, in *Proc. of 24th ICRC (Rome, Italy)*, Vol. 1 (1995) p. 399 .

[24] J. Allison *et al.*, Nucl. Instr. and Meth. A **835**, 186 (2016).

[25] Y. Asaoka *et al.* (CALET), Astroparticle Physics **100**, 29 (2018); Astroparticle Physics **91**, 1 (2017) .

[26] O. Adriani *et al.* (CALET), Phys. Rev. Lett. **129**, 251103 (2022).

[27] G. D'Agostini, Nucl. Instr. and Meth. A **362**, 487 (1995); T. Adye, (2011), arXiv:1105.1160 .

[28] A. Panov *et al.* (ATIC), Bull. Russian Acad. Sci. **73**, 564 (2009).

[29] H. S. Ahn *et al.* (CREAM), Astrophys. J. **707**, 593 (2009).

[30] O. Adriani *et al.* (CALET), Phys. Rev. Lett. **126**, 241101 (2021).

[31] W. R. Webber, and J. C. Kish, and D. A. Schrier, Phys. Rev. C **41**, 520 (1990); Phys. Rev. C **41**, 566 (1990) .

Full Author List: CALET Collaboration

O. Adriani[1,2], Y. Akaike[3,4], K. Asano[5], Y. Asaoka[5], E. Berti[2,6], G. Bigongiari[7,8], W.R. Binns[9], M. Bongi[1,2], P. Brogi[7,8], A. Bruno[10], N. Cannady[11,12,13], G. Castellini[6], C. Checchia[7,8], M.L. Cherry[14], G. Collazuol[15,16], G.A. de Nolfo[10], K. Ebisawa[17], A.W. Ficklin[14], H. Fuke[17], S. Gonzi[1,2,6], T.G. Guzik[14], T. Hams[11], K. Hibino[18], M. Ichimura[19], K. Ioka[20], W. Ishizaki[5], M.H. Israel[9], K. Kasahara[21], J. Kataoka[22], R. Kataoka[23], Y. Katayose[24], C. Kato[25], N. Kawanaka[20], Y. Kawakubo[14], K. Kobayashi[3,4], K. Kohri[26], H.S. Krawczynski[9], J.F. Krizmanic[12], P. Maestro[7,8], P.S. Marrocchesi[7,8], A.M. Messineo[8,27], J.W. Mitchell[12], S. Miyake[28], A.A. Moiseev[29,12,13], M. Mori[30], N. Mori[2], H.M. Motz[31], K. Munakata[25], S. Nakahira[17], J. Nishimura[17], S. Okuno[18], J.F. Ormes[32], S. Ozawa[33], L. Pacini[2,6], P. Papini[2], B.F. Rauch[9], S.B. Ricciarini[2,6], K. Sakai[11,12,13], T. Sakamoto[34], M. Sasaki[29,12,13], Y. Shimizu[18], A. Shiomi[35], P. Spillantini[1], F. Stolzi[7,8], S. Sugita[34], A. Sulaj[7,8], M. Takita[5], T. Tamura[18], T. Terasawa[5], S. Torii[3], Y. Tsunesada[36,37], Y. Uchihori[38], E. Vannuccini[2], J.P. Wefel[14], K. Yamaoka[39], S. Yanagita[40], A. Yoshida[34], K. Yoshida[21], and W.V. Zober[9]

[1]Department of Physics, University of Florence, Via Sansone, 1 - 50019, Sesto Fiorentino, Italy, [2]INFN Sezione di Firenze, Via Sansone, 1 - 50019, Sesto Fiorentino, Italy, [3]Waseda Research Institute for Science and Engineering, Waseda University, 17 Kikuicho, Shinjuku, Tokyo 162-0044, Japan, [4]JEM Utilization Center, Human Spaceflight Technology Directorate, Japan Aerospace Exploration Agency, 2-1-1 Sengen, Tsukuba, Ibaraki 305-8505, Japan, [5]Institute for Cosmic Ray Research, The University of Tokyo, 5-1-5 Kashiwa-no-Ha, Kashiwa, Chiba 277-8582, Japan, [6]Institute of Applied Physics (IFAC), National Research Council (CNR), Via Madonna del Piano, 10, 50019, Sesto Fiorentino, Italy, [7]Department of Physical Sciences, Earth and Environment, University of Siena, via Roma 56, 53100 Siena, Italy, [8]INFN Sezione di Pisa, Polo Fibonacci, Largo B. Pontecorvo, 3 - 56127 Pisa, Italy, [9]Department of Physics and McDonnell Center for the Space Sciences, Washington University, One Brookings Drive, St. Louis, Missouri 63130-4899, USA, [10]Heliospheric Physics Laboratory, NASA/GSFC, Greenbelt, Maryland 20771, USA, [11]Center for Space Sciences and Technology, University of Maryland, Baltimore County, 1000 Hilltop Circle, Baltimore, Maryland 21250, USA, [12]Astroparticle Physics Laboratory, NASA/GSFC, Greenbelt, Maryland 20771, USA, [13]Center for Research and Exploration in Space Sciences and Technology, NASA/GSFC, Greenbelt, Maryland 20771, USA, [14]Department of Physics and Astronomy, Louisiana State University, 202 Nicholson Hall, Baton Rouge, Louisiana 70803, USA, [15]Department of Physics and Astronomy, University of Padova, Via Marzolo, 8, 35131 Padova, Italy, [16]INFN Sezione di Padova, Via Marzolo, 8, 35131 Padova, Italy, [17]Institute of Space and Astronautical Science, Japan Aerospace Exploration Agency, 3-1-1 Yoshinodai, Chuo, Sagamihara, Kanagawa 252-5210, Japan, [18]Kanagawa University, 3-27-1 Rokkakubashi, Kanagawa, Yokohama, Kanagawa 221-8686, Japan, [19]Faculty of Science and Technology, Graduate School of Science and Technology, Hirosaki University, 3, Bunkyo, Hirosaki, Aomori 036-8561, Japan, [20]Yukawa Institute for Theoretical Physics, Kyoto University, Kitashirakawa Oiwake-cho, Sakyo-ku, Kyoto, 606-8502, Japan, [21]Department of Electronic Information Systems, Shibaura Institute of Technology, 307 Fukasaku, Minuma, Saitama 337-8570, Japan, [22]School of Advanced Science and Engineering, Waseda University, 3-4-1 Okubo, Shinjuku, Tokyo 169-8555, Japan, [23]National Institute of Polar Research, 10-3, Midori-cho, Tachikawa, Tokyo 190-8518, Japan, [24]Faculty of Engineering, Division of Intelligent Systems Engineering, Yokohama National University, 79-5 Tokiwadai, Hodogaya, Yokohama 240-8501, Japan, [25]Faculty of Science, Shinshu University, 3-1-1 Asahi, Matsumoto, Nagano 390-8621, Japan, [26]Institute of Particle and Nuclear Studies, High Energy Accelerator Research Organization, 1-1 Oho, Tsukuba, Ibaraki, 305-0801, Japan, [27]University of Pisa, Polo Fibonacci, Largo B. Pontecorvo, 3 - 56127 Pisa, Italy, [28]Department of Electrical and Electronic Systems Engineering, National Institute of Technology (KOSEN), Ibaraki College, 866 Nakane, Hitachinaka, Ibaraki 312-8508, Japan, [29]Department of Astronomy, University of Maryland, College Park, Maryland 20742, USA, [30]Department of Physical Sciences, College of Science and Engineering, Ritsumeikan University, Shiga 525-8577, Japan, [31]Faculty of Science and Engineering, Global Center for Science and Engineering, Waseda University, 3-4-1 Okubo, Shinjuku, Tokyo 169-8555, Japan, [32]Department of Physics and Astronomy, University of Denver, Physics Building, Room 211, 2112 East Wesley Avenue, Denver, Colorado 80208-6900, USA, [33]Quantum ICT Advanced Development Center, National Institute of Information and Communications Technology, 4-2-1 Nukui-Kitamachi, Koganei, Tokyo 184-8795, Japan, [34]College of Science and Engineering, Department of Physics and Mathematics, Aoyama Gakuin University, 5-10-1 Fuchinobe, Chuo, Sagamihara, Kanagawa 252-5258, Japan, [35]College of Industrial Technology, Nihon University, 1-2-1 Izumi, Narashino, Chiba 275-8575, Japan, [36]Graduate School of Science, Osaka Metropolitan University, Sugimoto, Sumiyoshi, Osaka 558-8585, Japan, [37]Nambu Yoichiro Institute for Theoretical and Experimental Physics, Osaka Metropolitan University, Sugimoto, Sumiyoshi, Osaka 558-8585, Japan, [38]National Institutes for Quantum and Radiation Science and Technology, 4-9-1 Anagawa, Inage, Chiba 263-8555, Japan, [39]Nagoya University, Furo, Chikusa, Nagoya 464-8601, Japan, [40]College of Science, Ibaraki University, 2-1-1 Bunkyo, Mito, Ibaraki 310-8512, Japan

PoS(ICRC2023)058